Journal of Power Sources 195 (2010) 5966–5970

Contents lists available at ScienceDirect

Journal of Power Sources

journal homepage: www.elsevier.com/locate/jpowsour

Short communication

Anodic Pt dissolution in concentrated trifluoromethanesulfonic acid

So Takizawa, Akira Nakazawa, Mitsuhiro Inoue, Minoru Umeda*

Department of Materials Science and Technology, Faculty of Engineering, Nagaoka University of Technology, Kamitomioka 1603-1, Nagaoka, Niigata 940-2188, Japan

ARTICLE INFO

Article history:
Received 30 September 2009
Received in revised form
12 November 2009
Accepted 14 December 2009
Available online 21 December 2009

Keywords:
Anodic Pt dissolution
Concentrated trifluoromethanesulfonic acid
Pt dual microelectrode
Potential step technique

ABSTRACT

We investigated the anodic Pt dissolution in concentrated trifluoromethanesulfonic acid (TFMSA). The dependence of the Pt dissolution rate on the TFMSA concentration was first measured from the weight difference of a Pt-flag electrode before and after successive potential cycles. From this measurement, the Pt dissolution rate in 10 mol dm^{-3} TFMSA is found to be over 40 times greater than those in 1 and 4 mol dm^{-3} TFMSA. Next, the anodic Pt dissolution was assessed in 10 mol dm^{-3} TFMSA by a potential step technique using a Pt dual microelectrode having generator and collector electrodes. The obtained result shows that the anodic Pt dissolution in 10 mol dm^{-3} TFMSA occurs when the Pt generator electrode potential is stepped from 0.25 to 1.0–2.0 V vs. Ag/Ag_2SO_4. Furthermore, the absolute steady-state current-based coulomb charges obtained at the generator ($|Q_G|$) and collector ($|Q_C|$) reflect the anodic Pt dissolution and the reduction of the dissolved Pt, respectively. The magnitude of $|Q_G|$ and $|Q_C|$ linearly increase when the generator potential shifts from 1.0 to 2.0 V vs. Ag/Ag_2SO_4. The absolute ratio, $|Q_C/Q_G|$, also gradually increases according to the shift in the generator electrode potential. These results demonstrate that the anodic Pt dissolution in 10 mol dm^{-3} TFMSA occurs at $\geq$1.0 V vs. Ag/Ag_2SO_4 and that the ratio of the anodic Pt dissolution per total reaction charges increases according to the positive shift of the Pt electrode potential.

1. Introduction

The polymer electrolyte fuel cell (PEFC) is a highly efficient power-generation system incorporating a poly(perfluoroalkylsulfonic acid) as the electrolyte membrane. In the PEFC, a Pt-based electrocatalyst, which is believed to be a non-corrosive material, is generally used for the cathode [1,2]. However, during the long-term operation of PEFC, the Pt included in the cathode catalyst gradually degrades [3,4]. This phenomenon includes a decrease in the effective surface area of the Pt catalysts [5,6], which leads to a decrease in the generating power.

Based on these results, it is inevitable to understand the detailed Pt dissolution phenomenon for suppressing the decreasing PEFC power generation. Many researchers have already investigated the Pt dissolution in acidic aqueous solutions [7–14]. For example, Pt has been reported to dissolve in a dilute H_2SO_4 during potential cycling [7–10,14]. In this case, two types of Pt dissolutions, namely, (i) a direct anodic Pt dissolution and (ii) a Pt dissolution during the re-reduction of Pt-oxide have been described to occur [8,9]. Thus, if details of the anodic and cathodic Pt dissolutions are clarified, a lasting long PEFC is expected.

Recently, we reported the Pt dissolution in concentrated H_2SO_4 solutions [15,16]. In the concentrated H_2SO_4, the Pt dissolution has been found to occur at a high rate when compared to that in dilute H_2SO_4 solutions. A cathodic Pt dissolution mechanism for the reduction of Pt-oxide has been realized by rotating ring-disk electrode (RRDE) and electrochemical quartz crystal microbalance (EQCM) techniques [16]. However, the details of the anodic Pt dissolution mechanism are still uncertain because the anodic Pt dissolution is not clearly observed in the concentrated H_2SO_4. This is because competitive reactions such as sulfur deposition and its reduction occur. Therefore, an electrolytic solution, which has the same kind of chemical structure as the perfluoroalkylsulfonic acid, is required for use in the anodic Pt dissolution study.

We focused our attention on the Pt dissolution during anodic polarization in concentrated trifluoromethanesulfonic acid (TFMSA), which has the same kind of chemical structure of the perfluoroalkylsulfonic acid. First, to investigate a high-rate Pt dissolution, the relationship between the TFMSA concentration and the amount of Pt dissolution was assessed by successive potential cycles. Based on this result, the electrode potential dependence of the anodic Pt dissolution was investigated in 10 mol dm^{-3} TFMSA in which the high-rate Pt dissolution occurs. In these experiments, a Pt dual microelectrode was used to catch the dissolved Pt.

2. Experimental

Electrochemical measurements were conducted using a three-compartment glass cell. A Pt-flag [17,18] and a Pt dual microelectrode [19,20] were used as the working electrodes. A Pt

* Corresponding author. Tel.: +81 258 47 9323; fax: +81 258 47 9323.
E-mail address: mumeda@vos.nagaokaut.ac.jp (M. Umeda).

0378-7753/$ – see front matter © 2009 Elsevier B.V. All rights reserved.
doi:10.1016/j.jpowsour.2009.12.055

plate and Ag/Ag_2SO_4 [15,16] were used as the counter and reference electrodes, respectively. The reference electrode was prepared as follows [16]. The surface of a Ag wire (Ø0.5 mm) was covered with Ag_2SO_4 by anodic polarization in 0.5 mol dm^{-3} H_2SO_4. A Pt wire of 100 μm diameter and 5 mm length was inserted inside of the tip of the glass tube for a liquid junction to the reference electrode. Subsequently, the tip of the glass tube was heat-sealed. Finally, the glass tube for the reference electrode including a silver wire, of which the surface was covered with Ag_2SO_4, was filled with saturated K_2SO_4 aqueous solution. The electrode potential of the prepared Ag/Ag_2SO_4 reference electrode was +0.744 V vs. SHE. TFMSA (Nacalai Tesque) diluted by Millipore water was used as the electrolytic solution. All the electrochemical measurements were conducted under deaerated conditions at 25 ± 1 °C.

The Pt dissolution in the TFMSA solutions was measured from the weight change of a Pt electrode before and after successive potential cycles at the sweep rate of 50 mV s^{-1} for 3 h. The experimental procedure is described as follows [15,16]. The electrochemical experiment was conducted by controlling the electrode potential using a potentiostat (Model 600, ALS). A Pt-flag electrode used as the working electrode was prepared as follows. A Pt plate (diameter: 5 mm, thickness: 0.03 mm) was connected with a Pt wire (Ø0.3 mm) by spot welding. Before use, the Pt-flag electrode was pretreated by potential cycling between −0.7 and +0.8 V vs. Ag/Ag_2SO_4 at a rate of 100 mV s^{-1} for 15 min in 0.5 mol dm^{-3} H_2SO_4. The profile of the obtained cyclic voltammogram was identical to the reported profile [21], which ensured that the Pt electrode surface was clean. The weight of the electrode before and after the successive potential cycles was measured by a microbalance (MX5, Mettler Toledo). For the measurement of the electrode weight after the potential cycles, the Pt-flag electrode was taken out from the electrochemical instrument, and then carefully washed with pure water and dried in a vacuum chamber at room temperature. From the difference of the Pt-flag electrode weight before and after the potential cycles, the Pt dissolution rate was determined.

Next, the anodic Pt dissolution was investigated using a Pt dual microelectrode as shown in Fig. 1. The Pt dual microelectrode was prepared as follows [19,20]. First, a theta glass capillary (TGC150-10, Harvard Apparatus) was pulled by a pipette puller (Model PN-30, Narishige) to obtain a thin septum thickness of theta glass so that the two Pt electrodes could be closely placed. The theta glass performs as an electric insulator for the two Pt wires. Ø50 and Ø20 μm Pt wires used as the generator and collector were separately inserted into the capillary and then heat-sealed by decompressing the glass inside. By using emery papers (#800–1000) and lapping films (#2000–4000), the tip of the Pt dual microelectrode was polished to a mirror finish. As seen from the photograph of the tip of the prepared Pt dual microelectrode (Fig. 1), the distance between the generator and collector is 40 μm. The Pt electrodes in the dual microelectrode were electrochemically cleaned in the same manner as that for the pretreatment of the Pt-flag electrode, subsequently, the anodic Pt dissolution was investigated in 10 mol dm^{-3} TFMSA. The electrode potential with respect to the Ag/Ag_2SO_4 reference electrode was controlled by a dual potentiostat (Model 700B, ALS). It should be noted that the collection efficiency of the prepared Pt dual microelectrode was 11.9%, which was determined by using 4 mmol dm^{-3} $K_4Fe(CN)_6$.

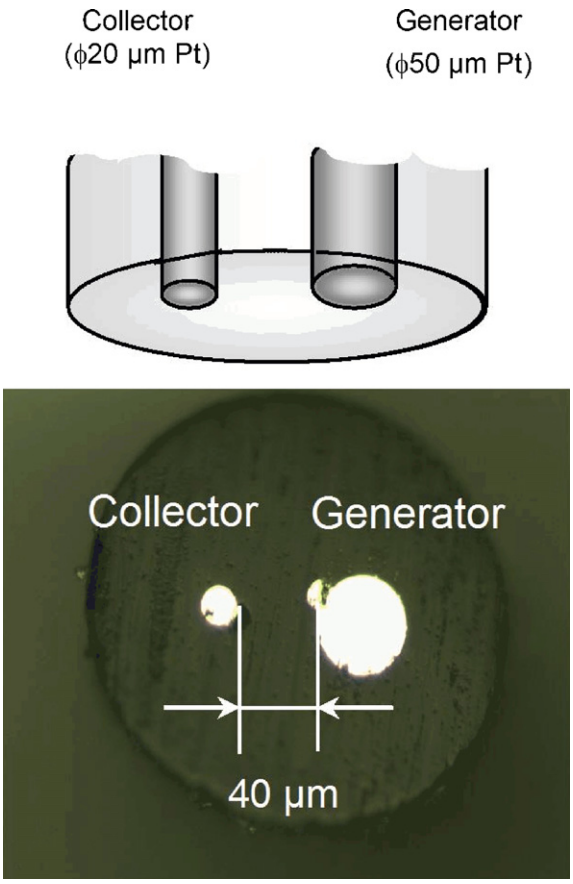

Fig. 1. Schematic diagram and photograph of the Pt dual microelectrode.

3. Results and discussion

3.1. Pt dissolution caused by successive potential cycles in various concentrations of TFMSA

First, cyclic voltammograms were measured in deaerated 1, 4, and 10 mol dm^{-3} TFMSA solutions at the sweep rate of 50 mV s^{-1}. The results obtained at the second potential sweep are shown in Fig. 2. In 1 and 4 mol dm^{-3} TFMSA solutions, typical cyclic voltammogram profiles of a Pt electrode in an acidic solution are observed [21]. In the case of the 10 mol dm^{-3} TFMSA, however, the potential window becomes wider and the anodic coulomb charge observed at 0.8–2.0 V vs. Ag/Ag_2SO_4 during the positive-going sweep decreases when compared to those in the 1 and 4 mol dm^{-3} TFMSA (see Table 1). This result suggests that a smaller amount of the Pt-oxide is formed on the Pt surface in the 10 mol dm^{-3} TFMSA [10]. It should be noted that the potential shift seen in Fig. 2 may be attributed to a change of the hydrogen electrode potential according to an increase in the TFMSA concentration [22].

Next, the amount of Pt dissolution in the TFMSA was measured from the weight difference of the Pt-flag electrode before and after the successive potential cycles in each TFMSA solution. The potential cycles were conducted between the anodic and cathodic edges of the potential windows as seen in Fig. 2. Table 1 represents the measured weight change rates of the Pt electrode. As for 1 and 4 mol dm^{-3} TFMSA, the Pt weight change rates are estimated to be less than -1 μg cm^{-2} h^{-1}. However, that obtained in the 10 mol dm^{-3} TFMSA is -40.8 μg cm^{-2} h^{-1}, which is over 40 times greater than that in 4 mol dm^{-3} TFMSA. In this case, competitive reactions which are observed in 18 mol dm^{-3} H_2SO_4 solution [15,16] does not occur. These results indicate the fact that the Pt easily dissolves in 10 mol dm^{-3} TFMSA without any competitive reaction, while it is still unclear whether the anodic or cathodic Pt dissolution mainly occurs. From Table 1, the Pt dissolution rate is also found to increase with decreasing in the coulomb charge of the Pt-oxide formation. According to this result, the drastic Pt dissolution in the 10 mol dm^{-3} TFMSA is considered to be related to the decrease in the amount of the Pt-oxide formation [12]. It should

Table 1
Weight change rates of Pt-flag electrode measured by successive potential cycles in TFMSA[a].

Concentration of TFMSA/mol dm^{-3}	Weight change rate/μg cm^{-2} h^{-1}	Charge amount of Pt-oxide formation[b]/mC
1	≈0	0.38
4	−0.85	0.42
10	−40.8	0.22

[a] The potential cycle was conducted in the potential window shown in Fig. 2 at a sweep rate of 50 mV s^{-1} for 3 h.
[b] These data were taken from the cyclic voltammograms shown in Fig. 2.

be noted that any Pt dissolved in the 10 mol dm^{-3} TFMSA was not detected by inductively coupled plasma spectrometer (SPS4000, Seiko).

3.2. Anodic Pt dissolution measured by the potential step technique in 10 mol dm^{-3} TFMSA

Based on the above results, the Pt dissolution easily occurs in the 10 mol dm^{-3} TFMSA. This high-rate Pt dissolution is similar to that reported in 16–18 mol dm^{-3} H_2SO_4 solutions [15,16]. In the case of the concentrated H_2SO_4, only the cathodic Pt dissolution mechanism has been represented by the RRDE and EQCM experimental results [16]. Therefore, the detailed anodic Pt dissolution is still uncertain. Thus, to investigate the anodic Pt dissolution, we focused our attention on the 10 mol dm^{-3} TFMSA in which the high-rate Pt dissolution occurs.

We have reported that the utilization of a Pt dual microelectrode makes it possible to observe reactions which were not measured by RRDE because the distance between the generator and collector electrodes is very close [20]. According to this, the anodic Pt dissolution in 10 mol dm^{-3} TFMSA was electrochemically measured by a potential step technique using a Pt dual microelectrode. The electrode potential of the generator was first held at 0.25 V vs. Ag/Ag_2SO_4 at which no electrode reaction occurs (see Fig. 2). Subsequently, the electrode potential was stepped to 2.0 V vs. Ag/Ag_2SO_4 which corresponds to the anodic edge of the potential window. Finally, the electrode potential was changed to 0.4 V vs. Ag/Ag_2SO_4 where the reduction of the Pt-oxide takes places. The potential holding time after the potential step was maintained at 10 s. The collector electrode potential was held at 0 V vs. Ag/Ag_2SO_4 during the measurement. Fig. 3 shows the current responses observed at the generator (upper) and the collector (lower). In the upper graph of Fig. 3, an anodic current, which consists of a transient current and a steady-state current, is observed when the Pt generator electrode potential is stepped from 0.25 to 2.0 V vs. Ag/Ag_2SO_4. At the same time, a cathodic current appears at the collector as seen in the lower portion of Fig. 3. However, during this collector current response, the magnitude of the steady-state current is high and that of the transient current is relatively low. At the collector electrode potential of 0 V vs. Ag/Ag_2SO_4, only the charge/discharge of the electrical double layer can be observed when no reactant is

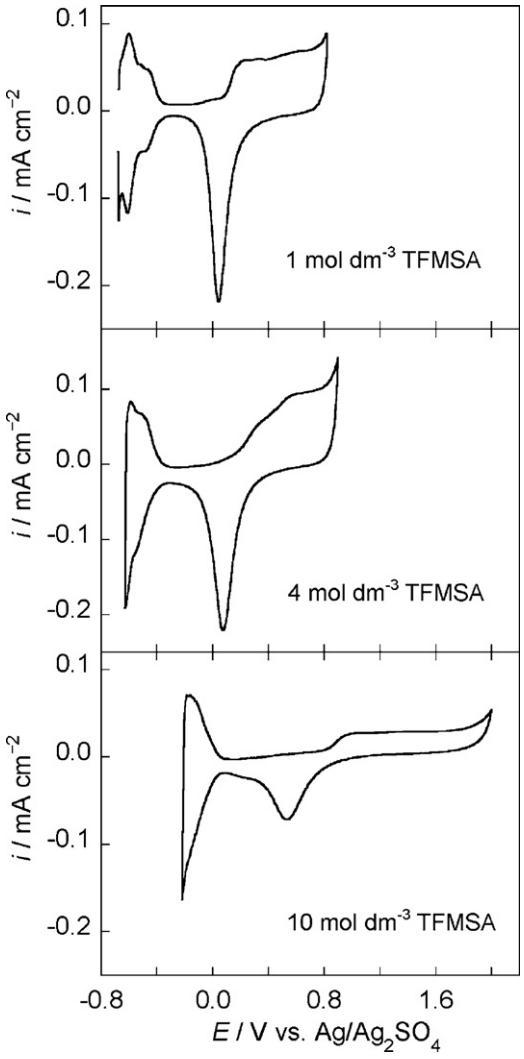

Fig. 2. Cyclic voltammograms of Pt-flag electrode (Ø5 mm) in 1, 4, and 10 mol dm^{-3} TFMSA. Sweep rate: 50 mV s^{-1}.

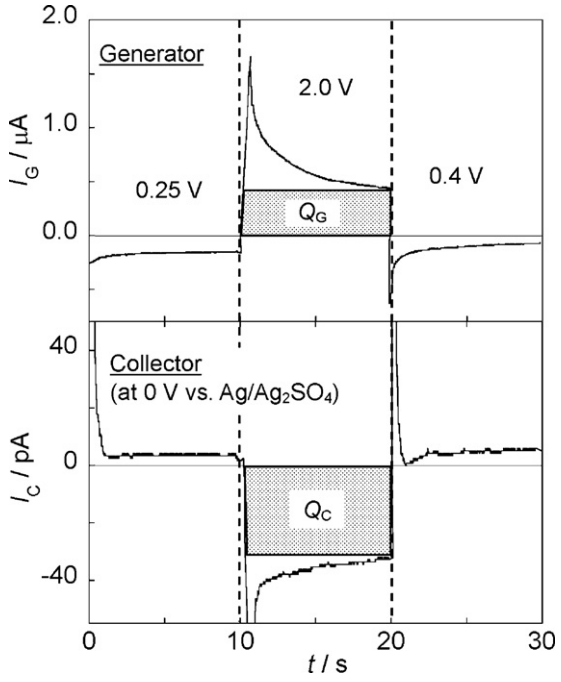

Fig. 3. Current responses at generator (upper) and collector (lower) obtained by stepping the generator potential in the order of 0.25, 2.0, 0.4 V vs. Ag/Ag_2SO_4 in the 10 mol dm^{-3} TFMSA. The collector potential was held at 0 V vs. Ag/Ag_2SO_4. Q_C and Q_G are explained in the text.

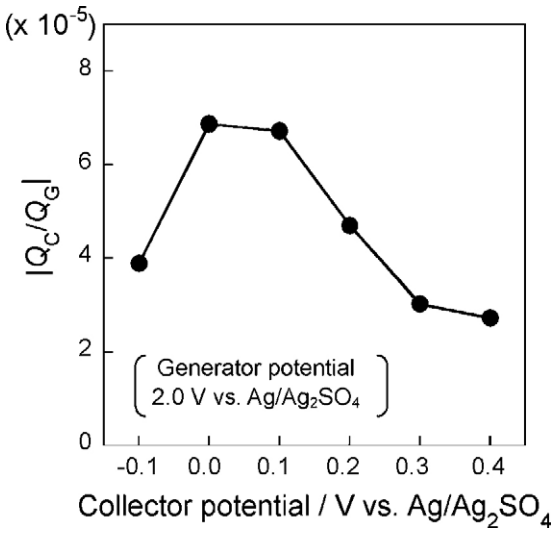

Fig. 4. Ratio of absolute coulomb charges obtained at generator (Q_G) and collector (Q_C) in 10 mol dm^{-3} TFMSA ($|Q_C/Q_G|$) as a function of the collector electrode potential. The generator electrode potential was held at 2.0 V vs. Ag/Ag$_2$SO$_4$ for 10 s.

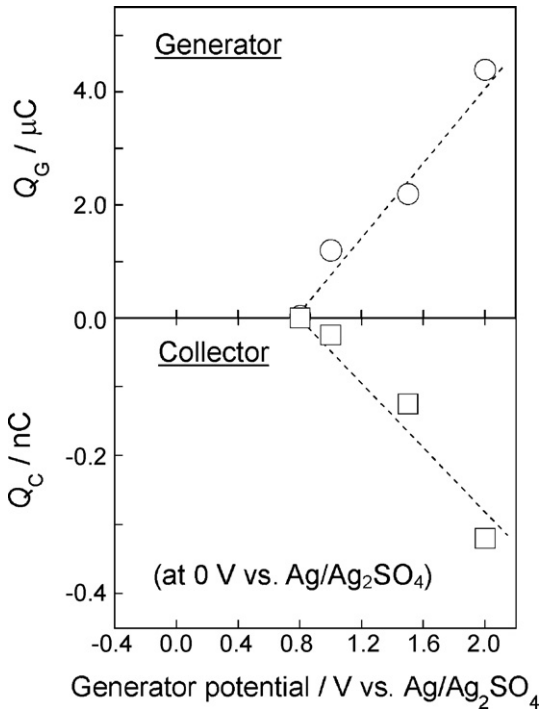

Fig. 5. Plots of coulomb charges measured at generator (Q_G) and collector (Q_C) in 10 mol dm^{-3} TFMSA as a function of the generator electrode potential in the second potential step. Potential holding time: 10 s. The collector electrode potential was held at 0 V vs. Ag/Ag$_2$SO$_4$.

included in the TFMSA (see Fig. 2). Therefore, the steady-state current obtained at the collector is considered to correspond to that at the generator. In other words, the steady-state current observed at the collector implies that a reactant is generated from the generator.

The steady-state current-based coulomb charges of Q_G and Q_C seen in Fig. 3 are also observed in the potential range of 1.0–2.0 V vs. Ag/Ag$_2$SO$_4$, as can be shown in the following Fig. 5. From the cyclic voltammogram of Fig. 2, it is obvious that no decomposition of the solvent occurs and only the Pt-oxide formation can be seen in the potential region. Based on this result, part of Q_G is considered to participate in the anodic Pt dissolution. Based on a Pt dissolution report, which was conducted by a stationary electrode potential holding for 72 h in 0.57 mol dm^{-3} HClO$_4$, the amount of the anodic Pt dissolution monotonically increases when the electrode potential shifts from 0.65 to 1.1 V vs. SHE, where the Pt-oxide formation also occurs [12]. Based on these results, the anodic Pt dissolution observed in the 10 mol dm^{-3} TFMSA can be considered to occur through the Pt-oxide formation.

3.3. Electrode potential dependence of anodic Pt dissolution

As realized from the above results, the anodic Pt dissolution from the generator is directly observed at the collector of the Pt dual microelectrode when the Pt generator potential is anodically polarized. Based on this result, the coulomb charges shown in the upper and lower graphs of Fig. 3 (Q_G and Q_C) are assumed to contain those of the anodic Pt dissolution and the reduction of the dissolved Pt, respectively. Based on this consideration, the electrode potential dependence of the anodic Pt dissolution could be investigated quantitatively from the magnitudes of the measured Q_G and Q_C.

First, to optimize the collector electrode potential to detect the dissolved Pt, the absolute ratio of Q_C and Q_G ($|Q_C/Q_G|$) was measured at various collector electrode potentials by fixing the generator electrode potential at 2.0 V vs. Ag/Ag$_2$SO$_4$. Fig. 4 shows the $|Q_C/Q_G|$ vs. the collector electrode potential. From the plots, the maximum $|Q_C/Q_G|$ value is observed at 0 V vs. Ag/Ag$_2$SO$_4$. This indicates that the anodically dissolved Pt can be efficiently reduced at 0 V vs. Ag/Ag$_2$SO$_4$, which is similar to the reported experimental result in 18 mol dm^{-3} H$_2$SO$_4$ that the dissolved Pt is reduced at around 0 V vs. Ag/Ag$_2$SO$_4$ [16]. Thus, the result from Fig. 4 supports the above-mentioned consideration that the anodic Pt dissolution occurs at the generator and the dissolved Pt is reduced at the collector. In the following experiment, the collector electrode potential was fixed at 0 V vs. Ag/Ag$_2$SO$_4$.

Next, the electrode potential dependence of the coulomb charge that originated during the anodic Pt dissolution was measured. The upper and lower graphs of Fig. 5 show Q_G and Q_C vs. the generator electrode potentials. Based on the figure, the magnitude of Q_G linearly increases when the generator electrode potential shifts from 0.8 to 2.0 V vs. Ag/Ag$_2$SO$_4$. According to the increase in Q_G, the magnitude of absolute Q_C linearly increases.

As mentioned above, a part of Q_G participates in the anodic Pt dissolution. Therefore, the absolute ratios of Q_C and Q_G ($|Q_C/Q_G|$)

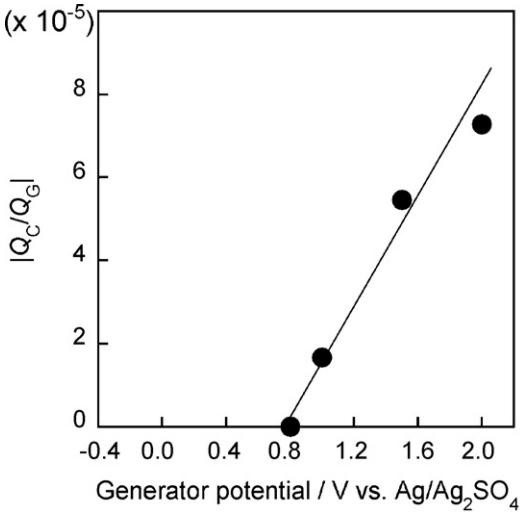

Fig. 6. Ratio of absolute coulomb charges ($|Q_C/Q_G|$) obtained from the plot in Fig. 5.

were calculated from the data of Fig. 5 to assess the extent of the Pt dissolution per total reaction charges. Fig. 6 shows the relationship between $|Q_C/Q_G|$ and the generator electrode potential. From the figure, the $|Q_C/Q_G|$ is known to increase as the generator electrode potential shifts in the positive direction. This result indicates that when the generator potential is much positive, the rate of the coulomb charge for the anodic Pt dissolution increases.

Consequently, the ratio of the anodic Pt dissolution in the 10 mol dm^{-3} TFMSA is found to depend on the electrode potential. The obtained results are worthwhile to understand the anodic Pt dissolution of the PEFC cathode which is believed to occur during the high-potential operation [23]. However, the anodic Pt dissolution mechanism remains unclear. In the future, we plan to investigate the anodic Pt dissolution mechanism.

4. Conclusions

In this study, we investigated the anodic Pt dissolution in TFMSA. The obtained results are summarized as follows:

(1) From the weight change of the Pt-flag electrode before and after successive potential cycles, the Pt dissolution rate in 10 mol dm^{-3} TFMSA is found to be over 40 times greater than those in 1 and 4 mol dm^{-3} TFMSA.
(2) Based on the results of the potential step measurement using the Pt dual microelectrode in 10 mol dm^{-3} TFMSA, the anodic Pt dissolution is known to occur when the generator electrode potential is stepped from 0.25 to 1.0–2.0 V vs. Ag/Ag_2SO_4.
(3) The absolute steady-state current-based coulomb charges obtained at the generator ($|Q_G|$) and collector ($|Q_C|$) linearly increase when the generator potential shifts from 1.0 to 2.0 V vs. Ag/Ag_2SO_4. Their absolute ratio $|Q_C/Q_G|$ also gradually increases according to the shift in the generator electrode potential. These results demonstrate that the anodic Pt dissolution in 10 mol dm^{-3} TFMSA occurs at $\geq$1.0 V vs. Ag/Ag_2SO_4 and that the ratio of the anodic Pt dissolution increases based on the positive shift in the Pt electrode potential.

Acknowledgement

This study was financially supported by the Research and Development of Polymer Electrolyte Fuel Cells Project from the New Energy and Industrial Technology Development Organization (NEDO), Japan.

References

[1] V. Mehta, J.S. Cooper, J. Power Sources 114 (2003) 32–53.
[2] S. Litster, G. McLean, J. Power Sources 130 (2004) 61–76.
[3] Y. Shao-Horn, W.C. Sheng, S. Chen, P.J. Ferreira, E.F. Holby, D. Morgan, Top. Catal. 46 (2007) 285–305.
[4] K. Sasaki, M. Shao, R. Adzic, in: F.N. Büchi, M. Inaba, T.J. Schmidt (Eds.), Polymer Electrolyte Fuel Cell Durability, Springer, New York, 2009, pp. 7–15.
[5] J. Xie, D.L. Wood III, K.L. More, P. Atanassov, R.L. Borup, J. Electrochem. Soc. 152 (2005) A1011–A1020.
[6] X. Yu, S. Ye, J. Power Sources 172 (2007) 145–154.
[7] K. Kinoshita, J.T. Lundquist, P. Stonehart, J. Electroanal. Chem. 48 (1973) 157–166.
[8] D.C. Johnson, D.T. Napp, S. Bruckenstein, Electrochim. Acta 15 (1970) 1493–1509.
[9] D.A.J. Rand, R. Woods, J. Electroanal. Chem. 35 (1972) 209–218.
[10] K. Ota, S. Nishigori, N. Kamiya, J. Electroanal. Chem. 257 (1988) 205–215.
[11] P.J. Ferreira, G.J. la O', Y. Shao-Horn, D. Morgan, R. Makharia, S. Kocha, H.A. Gasteiger, J. Electrochem. Soc. 152 (2005) A2256–A2271.
[12] X. Wang, R. Kumar, D.J. Myers, Electrochem. Solid-State Lett. 9 (2006) A225–A227.
[13] S. Mitsushima, S. Kawahara, K. Ota, N. Kamiya, J. Electrochem. Soc. 154 (2007) B153–B158.
[14] Y. Sugawara, A.P. Yadav, A. Nishikata, T. Tsuru, Electrochemistry 75 (2007) 359–365.
[15] F. Kodera, Y. Kuwahara, A. Nakazawa, M. Umeda, J. Power Sources 172 (2007) 698–703.
[16] M. Umeda, Y. Kuwahara, A. Nakazawa, M. Inoue, J. Phys. Chem. C 113 (2009) 15707–15713.
[17] M. Umeda, H. Ojima, M. Mohamedi, I. Uchida, J. Power Sources 136 (2004) 10–15.
[18] S. Tanaka, M. Umeda, H. Ojima, Y. Usui, O. Kimura, I. Uchida, J. Power Sources 152 (2005) 34–39.
[19] M. Umeda, A. Kabasawa, M. Kokubo, M. Mohamedi, T. Itoh, I. Uchida, Jpn. J. Appl. Phys. 40 (2001) 5141–5144.
[20] K. Kashima, M. Umeda, A. Yamada, I. Uchida, Chem. Lett. 33 (2004) 1622–1623.
[21] A.J. Bard, L.R. Faulkner, Electrochemical Methods: Fundamentals and Applications, 2nd ed., Wiley, New York, 2001, p. 570.
[22] H.S. Harned, W.J. Hamer, J. Am. Chem. Soc. 57 (1935) 27–33.
[23] T. Yoda, H. Uchida, M. Watanabe, Electrochim. Acta 52 (2007) 5997–6005.